minerals

MDPI

Article

Fiemmeite $Cu_2(C_2O_4)(OH)_2 \cdot 2H_2O$, a New Mineral from Val di Fiemme, Trentino, Italy

Francesco Demartin [1,*], Italo Campostrini [1], Paolo Ferretti [2] and Ivano Rocchetti [2]

[1] Dipartimento di Chimica, Università degli Studi di Milano, Via C. Golgi 19, I-20133 Milano, Italy; italo.campostrini@unimi.it

[2] MUSE, Museo delle Scienze di Trento, Corso del Lavoro e della Scienza 3, I-38122 Trento, Italy; paolo.ferretti@muse.it (P.F.); ivanorocchetti@tiscali.it (I.R.)

* Correspondence: francesco.demartin@unimi.it; Tel.: +39-02-503-14457

Received: 28 May 2018; Accepted: 11 June 2018; Published: 12 June 2018

Abstract: The new mineral species fiemmeite, $Cu_2(C_2O_4)(OH)_2 \cdot 2H_2O$, was found NE of the Passo di San Lugano, Val di Fiemme, Carano, Trento, Italy (latitude 46.312° N, longitude 11.406° E). It occurs in coalified woods at the base of the Val Gardena Sandstone (upper Permian) which were permeated by mineralizing solutions containing Cu, U, As, Pb and Zn. The oxalate anions have originated from diagenesis of the plant remains included in sandstones. The mineral forms aggregate up to 1 mm across of sky blue platelets with single crystals reaching maximum dimensions of about 50 μm. Associated minerals are: baryte, olivenite, middlebackite, moolooite, brochantite, cuprite, devilline, malachite, azurite, zeunerite/metazeunerite, tennantite, chalcocite, galena. Fiemmeite is monoclinic, space group: $P2_1/c$ with a = 3.4245(6), b = 10.141(2), c = 19.397(3) Å, β = 90.71(1)°, V = 673.6(2) Å^3, Z = 4. The calculated density is 2.802 g/cm^3 while the observed density is 2.78(1) g/cm^3. The six strongest reflections in the X-ray powder diffraction pattern are: [d_{obs} in Å (I)(hkl)] 5.079(100)(020), 3.072(58)(112), 9.71(55)(002), 4.501(50)(022), 7.02(28)(012), 2.686(25)(114). The crystal structure was refined from single-crystal data to a final R_1 = 0.0386 for 1942 observed reflections [$I > 2\sigma(I)$] with all the hydrogen atoms located from a Difference–Fourier map. The asymmetric unit contains two independent Cu^{2+} cations that display a distorted square-bipyramidal (4+2) coordination, one oxalate anion, two hydroxyl anions and two water molecules. The coordination polyhedra of the two copper atoms share common edges to form polymeric rows running along [100] with composition $[Cu_2(C_2O_4)(OH)_2 \cdot 2H_2O]_n$. These rows are held together by a well-established pattern of hydrogen bonds between the oxalate oxygens not involved in the coordination to copper, the hydrogen atoms of the water molecules and the hydroxyl anions.

Keywords: fiemmeite; new oxalate mineral; Val di Fiemme; Trentino; Italy

1. Introduction

The presence of small Cu ore deposits, in the area close to the Passo di San Lugano, Val di Fiemme, Carano, Trento, Italy is well known since the XV and XVI century, as documented by the remains of the old mining sites. From a stratigraphic point of view, the deposits are located within the Val Gardena Sandstone (upper Permian) a few meters above the limit with the ignimbrites of the Athesian Volcanic Group (lower Permian). The sedimentary sequence of the upper Permian consists of the continental deposits of alluvial plain of the Val Gardena Sandstone. The unconformity at the base of the Val Gardena Sandstone indicates a prolonged sub-aerial exposure with erosion of the volcanic substrate and consequent articulated topography. In this context, the deposition of the Val Gardena Sandstone began, in an environment of alluvial plain. The basal portion of the Val Gardena Sandstone corresponds to the first of the five third-order depositional sequences identified by Massari et al. [1],

and is represented mainly by deposits of alternating alluvial conoids and reddened mudstones with pedogenized horizons and evaporites. The mineralization is set at the height of a Cu and U rich level, located at the base of the Val Gardena Sandstone (upper Permian). The major ore concentrations are found in deposits of carbon frustules and especially inside coalified trunks of up to metric sizes, impregnated with framboidal pyrite, covellite, tennantite and uraninite and surrounded by evident colored halos of supergenic minerals. This mineralization, referable to "sandstone-uranium type" deposits, can be explained by a genetic model given by a continental source made up of granite or acid volcanites that are eroded in an arid continental climate and then transported with U and other heavy metals, such as Cu, Pb, Zn, in the form of ions dissolved in clastic aquifers, in our case the alluvial conoid deposits of the Val Gardena Sandstone. The deposition of these ions is due to the strong decrease in solubility resulting from the reaction between mineralized groundwater and the strongly reducing environment given by the accumulation of trunks and organic matter in the channels or deposits of overbank. The peculiar greyish color of the sandstones for a range of a few meters around the levels with coalified trunks is a typical example of a reduction front (roll front) [2]. In this environment (latitude 46.312° N, longitude 11.406° E) we have recently identified the second world occurrence of middlebackite $Cu_2C_2O_4(OH)_2$ [3], a new copper oxalate discovered at the Iron Monarch quarry, Middleback Range, Australia and approved by the IMA CNMNC in 2016 (IMA 2015-115) [4]. A systematic investigation by micro-Raman spectroscopy of the mineralogical phases deposited (see Appendix A), allowed us to recognize that, besides middlebackite, other copper oxalates were present such as moolooite $CuC_2O_4 \cdot H_2O$ and another new mineral with chemical formula $Cu_2(C_2O_4)(OH)_2 \cdot 2H_2O$, that was approved as a new species by the IMA Commission on New Minerals, Nomenclature and Classification (No. 2017-115) with the name fiemmeite, after the type locality where it was found. This paper deals with the description of the new mineral fiemmeite, together with its crystal structure determination. Holotype material of fiemmeite is deposited in the Reference Collection of MUSE, Museo delle Scienze di Trento, sample No. 5249.

2. Experimental Data

2.1. Mineral Description and Physical Properties

Fiemmeite occurs in coalified woods as aggregates up to 1 mm across (Figure 1) made of sky blue elongated platelets with maximum dimensions about 50 μm. Associated minerals are: baryte, olivenite, middlebackite, moolooite, brochantite, cuprite, devilline, malachite, azurite, zeunerite/metazeunerite, tennantite, chalcocite and galena. The streak is pale blue and the lustre is from vitreous to waxy. It is brittle with cleavage almost perfect parallel to {010} or {001}, according to the weakest bonds observed in the crystal structure, and fracture uneven in the other directions. Its hardness was not determined due to the minute size of the crystals. Twinning was not observed. The mineral is non-fluorescent both under long- and short-wave ultraviolet radiation. A measurement of the density, obtained by flotation in a diiodomethane-benzene mixture gives the value of 2.78(1) g/cm^3. The density calculated using the empirical formula and single-crystal unit-cell data is 2.802 g/cm^3.

Crystals appear as highly birefringent platelets but we could not perform a precise optical characterization. The maximum and minimum refractive index we could measure are 1.90 and 1.54. A Gladstone-Dale calculation using the data of Mandarino [5,6] gives a mean refractive index of 1.64.

Figure 1. Fiemmeite aggregates with olivenite on coalified wood (base width 4 mm).

2.2. Chemical Data

Insufficient material is available for a direct determination of H_2O or C_2O_3 with a CHN analyzer. The presence of H_2O and C_2O_3 was confirmed by crystal structure analysis and Raman spectroscopy. Crystals rapidly decompose under a microprobe electron beam even using a low voltage current and a wide electron beam, therefore quantitative determination of Cu by microprobe analysis was not possible. However five chemical analyses of the copper and zinc content could be carried out, before damage of the sample, by means of a JEOL JSM 5500LV electron microscope equipped with an IXRF EDS 2000 microprobe (Table 1) with the following conditions: 20 kV, 10^{-11} A, 2 µm beam diameter. No other significant element quantities, besides Cu, Zn, O and C, were detected.

Table 1. Chemical data for fiemmeite.

Constituent	wt %	Range	Stand. Dev.	Probe Standard	wt % **
Cu	44.00	43.79–44.24	0.19	Synth. CuO	44.57
Zn	0.09	0.06–0.12	0.02	Synth. ZnO	0
O	44.40 *				44.89
C	8.34 *				8.42
H	2.10 *				2.12
Total	98.93				100.00

* theoretical for the empirical formula (based on 8 anions) $Cu_{1.996}Zn_{0.004}(C_2O_4)(OH)_2 \cdot 2H_2O$; ** theoretical for the empirical formula $Cu_2(C_2O_4)(OH)_2 \cdot 2H_2O$.

2.3. Micro Raman Spectroscopy

The Raman spectrum (Figure 2a,b) was obtained with an ANDOR 303 spectrometer equipped with a CCD camera iDus DV420A-OE, and with a Nikon CF plan 50×/0.55 objective. The 532 nm line of an OXXIUS solid state laser was used for excitation. The laser power was set to 10 mW in order to prevent damage of the crystal, with an aperture of 75 µm and 8.2 mm working distance. The two bands at 1683 and 1705 cm^{-1} can be assigned to ν_a(C=O), that at 1457 cm^{-1} to ν_s(C-O) + ν_s(C-C), that at 903 cm^{-1} to ν_s(C-O) + δ(O-C=O), that at 853 cm^{-1} to ν_s(C-O)/δ(O-C=O). Those at 466, 517 and 543 cm^{-1} are attributable to ν(Cu-O) + ν(C-C). The remaining below 298 cm^{-1} are assigned to out-of-plane bends and to lattice modes [7]. The observed bands at 3438 and 3471 cm^{-1} (Figure 2b) of

the OH/H_2O region are consistent with the range of hydrogen bond lengths found (2.655–2.903 Å), according to the Libowitzky correlation [8].

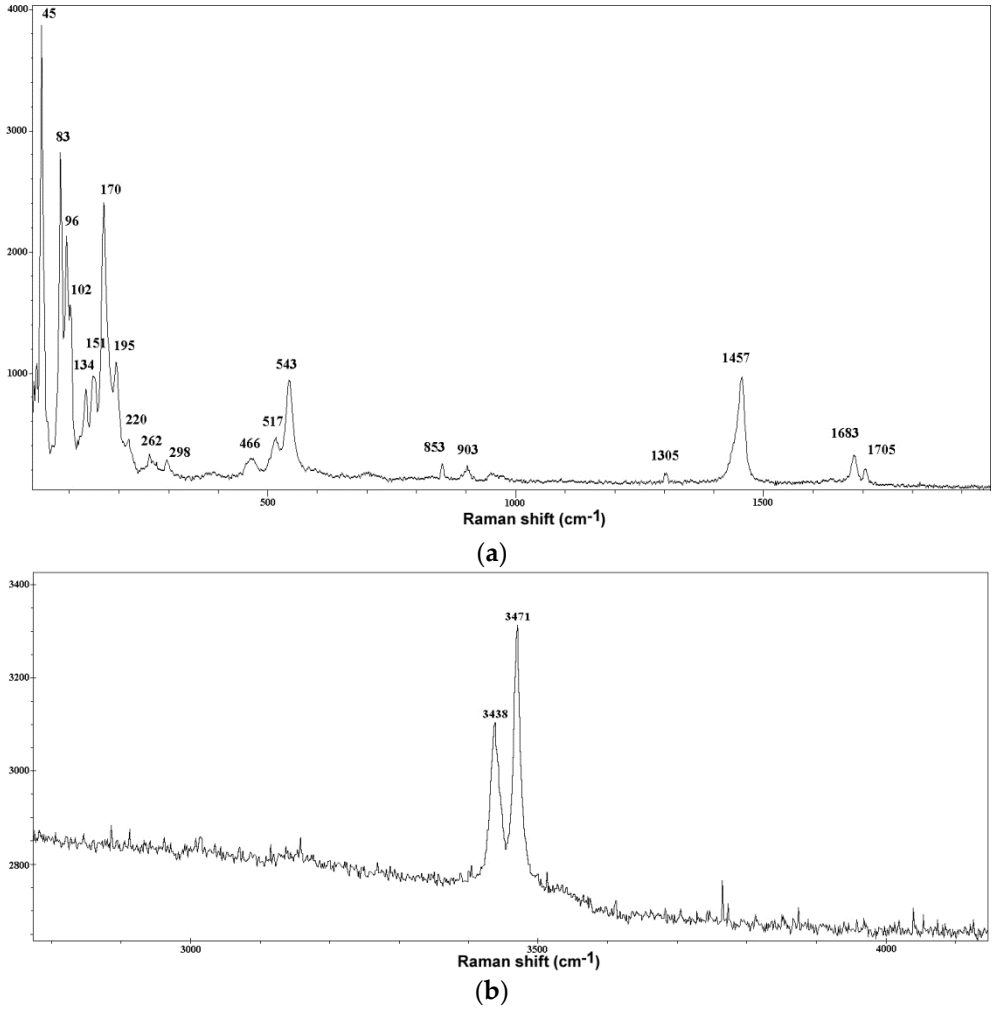

Figure 2. Micro-Raman spectrum of fiemmeite. (**a**) Oxalate and lattice mode bands; (**b**) hydrogen bond bands.

2.4. Crystallography

X-ray powder diffraction data of fiemmeite were obtained using a Bruker D8 diffractometer with graphite monochromatized CuKα radiation (Table 2). The unit-cell parameters, refined from powder data using the UNITCELL software [9], are: a = 3.4345(5), b = 10.159(2), c = 19.412(3) Å, β = 90.83(1)°, V = 677.5(1) Å^3.

Details of the single-crystal X-ray diffraction data collection and refinement are given in Table 3. 7512 intensities were collected at room temperature on a Bruker Apex II diffractometer with MoKα radiation (λ = 0.71073 Å) up to 2θ = 63.16°, of which 2118 unique. SADABS [10] absorption correction was applied. The structure was solved with direct methods [11] and refined with SHELXL-2017 [12] to a final R_1 = 0.0386 for 1942 observed reflections [$I > 2\sigma(I)$]. All the non-hydrogen atoms were refined anisotropically. All the hydrogen atoms were located in a Difference-Fourier map and refined. The coordinates and displacement parameters of the atoms are reported in Table 4; selected interatomic distances and angles and bond-valence values are listed in Table 5. The CIF file of fiemmeite is available as Supplementary Material.

Table 2. X-ray powder diffraction data for fiemmeite.

d_{obs} (Å)	I_{obs}	d_{calc} (Å) $^{\$}$	I_{calc} $^{\$}$	*h, k, l*	d_{obs} (Å)	I_{obs}	d_{calc} (Å) $^{\$}$	I_{calc} $^{\$}$	*h, k, l*
9.71	55	9.698	68	0 0 2	2.251	5	2.247	3	0 4 4
7.02	28	7.009	34	0 1 2	2.190	12	2.187	16	0 2 8
		5.452	3	0 1 3			2.162	6	−1 −3 4
5.079	100	5.071	100	0 2 0	2.151	13	2.147	17	1 3 4
4.914	12	4.906	10	0 2 1			2.122	3	1 2 6
4.855	2	4.849	5	0 0 4			2.052	1	−1 −3 5
4.501	50	4.493	40	0 2 2			2.036	2	1 3 5
3.996	4	3.990	6	0 2 3			2.028	6	−1 −4 1
		3.330	2	0 3 1			2.017	2	0 5 1
		3.241	4	−1 0 2			1.997	1	−1 −4 2
3.237	5	3.233	7	0 0 6	1.998	3	1.995	7	0 4 6
		3.193	1	−1 −1 1			1.972	1	1 2 7
3.198	5	3.192	7	0 3 2			1.953	1	−1 1 8
3.072	58	3.087	65	1 1 2	1.943	8	1.938	13	−1 3 6
3.001	2	2.996	6	0 3 3			1.935	4	0 5 3
2.891	20	2.886	18	1 1 3			1.905	3	0 1 10
		2.813	2	−1 0 4			1.883	2	−1 −4 4
		2.811	5	−1 −2 1			1.873	2	1 4 4
		2.731	2	−1 2 2	1.873	5	1.870	6	0 4 7
2.730	15	2.726	9	0 2 6			1.824	6	−1 3 7
		2.711	13	−1 −1 4			1.809	2	−1 −4 5
2.686	25	2.682	32	1 1 4			1.797	4	0 5 5
		2.608	2	−1 −2 3	1.755	7	1.752	10	0 4 8
		2.589	1	1 2 3			1.745	1	1 5 0
2.552	3	2.549	6	0 3 5			1.719	1	−1 −5 2
		2.514	1	0 4 1			1.716	3	1 5 2
2.511	2	2.503	6	−1 −1 5			1.697	2	−1 0 10
2.468	2	2.474	7	−1 −2 4	1.695	9	1.689	7	−2 0 2
		2.453	2	0 4 2			1.688	6	2 1 0
2.442	4	2.438	5	1 2 4			1.687	3	−1 −5 3
		2.431	3	0 2 7			1.666	2	−2−1 2
		2.424	1	0 0 8	1.657	3	1.656	6	1 1 10
		2.390	1	−1 −3 1			1.639	5	−1 −5 4
		2.360	2	0 4 3			1.642	4	0 4 9
		2.340	2	−1 −3 2			1.636	3	1 4 7
		2.336	3	0 3 6			1.609	3	−1 2 10
		2.336	2	1 0 6			1.603	4	−2 −2 2
		2.330	3	1 3 2			1.598	4	1 3 9
2.310	6	2.303	9	−1 1 6			1.596	2	0 6 4
		2.261	2	−1 −3 3			1.578	2	−2 −2 3
		2.248	4	1 3 3			1.544	3	−2 −2 4

Note: $^{\$}$ Pattern calculated on the basis of the single crystal data and structure refinement.

Table 3. Single-crystal diffraction data and refinement parameters for fiemmeite.

Crystal System	Monoclinic
Space Group	$P2_1/c$ (No. 14)
a (Å)	3.4245(6)
b (Å)	10.141(2)
c (Å)	19.397(3)
β (°)	90.71(1)
V (Å^3)	673.6(2)
Z	4
Radiation	Mo$K\alpha$ (λ = 0.71073 Å)
μ (mm^{-1})	6.322
D_{calc} (g·cm^{-3})	2.802
Measured reflections	7512
R_{int}	0.0294
Independent reflections	2118
Range of h, k, l	$-5 \leq h \leq 4$, $-14 \leq k \leq 14$, $-28 \leq l \leq 28$
Observed reflections [$I > 2\sigma(I)$]	1942
Parameters refined	133
Final R_1 [$I > 2\sigma(I)$] and $wR2$ (all data)	0.0386, 0.0905
GooF	1.176
Max/min residuals (e/Å^3)	1.37/−0.73

Notes: $R_1 = \Sigma||Fo| - |Fc||/\Sigma|Fo|$; $wR2 = \{\Sigma[w(Fo^2 - Fc^2)^2]/\Sigma[w(Fo^2)^2]\}^{1/2}$; $w = 1/[\sigma^2(Fo^2) + (0.0268q)^2 + 3.8682q]$ where $q = [\max(0, Fo^2) + 2Fc^2]/3$; GooF = $\{\Sigma[w(Fo^2 - Fc^2)]/(n - p)\}^{1/2}$ where n is the number of reflections and p is the number of refined parameters.

Table 4. Atom coordinates and displacement parameters [U_{eq}/U^{ij}, Å^2].

Atom	*x*/*a*	*y*/*b*	*z*/*c*	U_{eq}		
Cu1	0.19372(13)	0.24133(4)	0.50020(2)	0.0126(1)		
Cu2	0.61198(13)	0.29545(4)	0.37303(2)	0.0131(1)		
C1	0.0211(11)	0.1394(3)	0.6268(2)	0.0130(6)		
C2	−0.1380(10)	0.2827(4)	0.6259(2)	0.0132(6)		
O1	0.2069(8)	0.1067(3)	0.5731(1)	0.0160(5)		
O2	−0.1081(8)	0.3439(3)	0.5690(1)	0.0169(5)		
O3	−0.0369(9)	0.0695(3)	0.6773(1)	0.0228(6)		
O4	−0.2941(9)	0.3269(3)	0.6784(1)	0.0221(6)		
OH5	0.6196(7)	0.1665(2)	0.4475(1)	0.0130(5)		
OH6	0.1952(8)	0.3715(3)	0.4273(1)	0.0139(5)		
Ow7	0.9519(9)	0.1899(3)	0.3121(1)	0.0193(5)		
Ow8	0.5910(10)	0.4305(3)	0.3023(1)	0.0263(7)		
H5	0.666(16)	0.0765(16)	0.441(3)	0.032(15)		
H6	0.182(14)	0.4626(13)	0.434(3)	0.026(14)		
H71	0.861(16)	0.193(6)	0.2664(11)	0.037(16)		
H72	0.932(19)	0.0986(14)	0.318(3)	0.046(18)		
H81	0.706(17)	0.423(7)	0.2589(15)	0.047(19)		
H82	0.504(15)	0.517(2)	0.309(3)	0.028(14)		
Atom	U^{11}	U^{22}	U^{33}	U^{23}	U^{13}	U^{12}
Cu1	0.0151(2)	0.0118(2)	0.01106(19)	0.00217(14)	0.00295(14)	0.00301(15)
Cu2	0.0156(2)	0.0120(2)	0.01179(19)	0.00236(14)	0.00336(14)	0.00312(15)
C1	0.0148(15)	0.0107(14)	0.0137(14)	−0.0003(11)	0.0008(11)	0.0013(12)
C2	0.0096(14)	0.0151(15)	0.0149(15)	−0.0014(12)	−0.0002(11)	0.0009(12)
O1	0.0211(13)	0.0124(12)	0.0147(11)	0.0011(9)	0.0044(9)	0.0056(10)
O2	0.0236(14)	0.0124(12)	0.0147(11)	0.0019(9)	0.0056(9)	0.0053(10)
O3	0.0360(17)	0.0152(13)	0.0175(13)	0.0055(10)	0.0091(11)	0.0069(12)
O4	0.0328(16)	0.0182(13)	0.0155(12)	−0.0012(10)	0.0075(11)	0.0090(12)
OH5	0.0149(12)	0.0097(11)	0.0145(11)	0.0019(9)	0.0029(9)	0.0042(9)
OH6	0.0159(12)	0.0116(11)	0.0144(11)	0.0026(9)	0.0034(9)	0.0033(9)
Ow7	0.0301(15)	0.0139(12)	0.0141(12)	−0.0007(9)	0.0045(10)	0.0041(11)
Ow8	0.0406(18)	0.0192(14)	0.0194(13)	0.0079(11)	0.0132(12)	0.0133(13)

The anisotropic displacement factor exponent takes the form: $-2\pi^2(U^{11}h^2(a^*)^2 + ... + 2U^{12}hka^*b^* + ...)$; U_{eq} according to Fischer and Tillmans [13].

Table 5. Selected interatomic distances (Å), angles (°) and bond-valence sums (vu).

Atom1-Atom2	Distance	vu	Atom1-Atom2	Distance	vu
Cu1-OH6	1.935(3)	0.50	Cu2-Ow8	1.939(3)	0.46
Cu1-OH5	1.946(2)	0.46	Cu2-OH5	1.948(3)	0.45
Cu1-O1	1.966(3)	0.43	Cu2-OH6	1.943(3)	0.46
Cu1-O2	1.992(3)	0.40	Cu2-Ow7	1.983(3)	0.41
Cu1-OH5#1	2.332(3)	0.16	Cu2-OH6#2	2.375(3)	0.14
Cu1-O2#2	2.916(3)	0.03	Cu2-Ow7#1	2.754(3)	0.05
	Total	1.98		Total	1.97
Cu1-Cu2	2.9198(7)		C1-C2	1.552(5)	
C1-O3	1.228(4)		C2-O4	1.240(4)	
C1-O1	1.271(4)		C2-O2	1.270(4)	
Atom1-Atom2-Atom3	**angle**		**Atom1-Atom2-Atom3**	**angle**	
O1-C1-O3	126.2(3)		O1-C1-C2	114.5(3)	
C1-C2-O2	115.8(3)		O2-C2-O4	125.2(3)	
C1-C2-O4	118.9(3)		C2-C1-O3	119.3(3)	
Hydrogen bond interactions					
Atom1 ··· Atom2	**distance**		**Atom1-Atom2 ··· Atom3**	**angle**	
OH5 ··· O1#3	2.862(4)		OH5-H5 ··· O1#3	177(5)	
OH6 ··· O2#4	2.903(4)		OH6-H6 ··· O2#4	169(5)	
Ow7 ··· O3#3	2.655(4)		Ow7-H72 ··· O3#3	163(6)	
Ow7 ··· O4#5	2.722(4)		Ow7-H71 ··· O4#5	171(6)	
Ow8 ··· O4#4	2.691(4)		Ow8-H82 ··· O4#4	175(5)	
Ow8 ··· O3#5	2.753(4)		Ow8-H81 ··· O3#5	172(6)	

Symmetry codes: #1 = $x-1$,y,z; #2 = $x+1$,y,z; #3 = $1-x$, $-y$, $1-z$; #4 = $-x$, $1-y$, $1-z$; #5 = $x+1$, $1/2-y$, $z-1/2$. Bond-valence parameters after [14].

3. Crystal Structure Description and Discussion

The asymmetric unit of fiemmeite contains two independent Cu^{2+} cations, one oxalate anion, two hydroxyl anions and two water molecules (Figure 3a). Both copper cations display a distorted square-bipyramidal (4+2) coordination with four equatorial distances in the range 1.935(3)–1.992(3) Å, one apical distance intermediate [2.332(3)–2.375(3) Å] and one apical distance longer 2.754(3)–2.916(3) Å. Cu1 is coordinated by three oxygens of the oxalate anion and by three OH- anions. Cu2 is coordinated by three water molecules and by three OH^- anions.

The coordination polyhedra of the two copper atoms shares common edges to form polymeric rows, with composition $[Cu_2(C_2O_4)(OH)_2 \cdot 2H_2O]_n$, running along [100]. These rows are held together by a well-established pattern of hydrogen bonds (see Table 5) between the oxalate oxygens O3 and O4, not involved in the coordination to copper and the hydrogen atoms of the water molecules and between the other oxalate oxygens O1 and O2 and the hydroxyl anions.

Fiemmeite is the third example of oxalate containing only Cu^{2+} as cation, the others being moolooite $CuC_2O_4 \cdot H_2O$ [15], and middlebackite $Cu_2C_2O_4(OH)_2$ [4]. Other copper(II) oxalates with additional cations are wheatleyite $Na_2Cu(C_2O_4)_2 \cdot 2H_2O$ [16] and antipinite $KNa_3Cu_2(C_2O_4)_4$ [17].

A comparison of the crystal structure of fiemmeite with that of the other oxalates containing only copper can be done with middlebackite only, because the structure of moolooite is unknown.

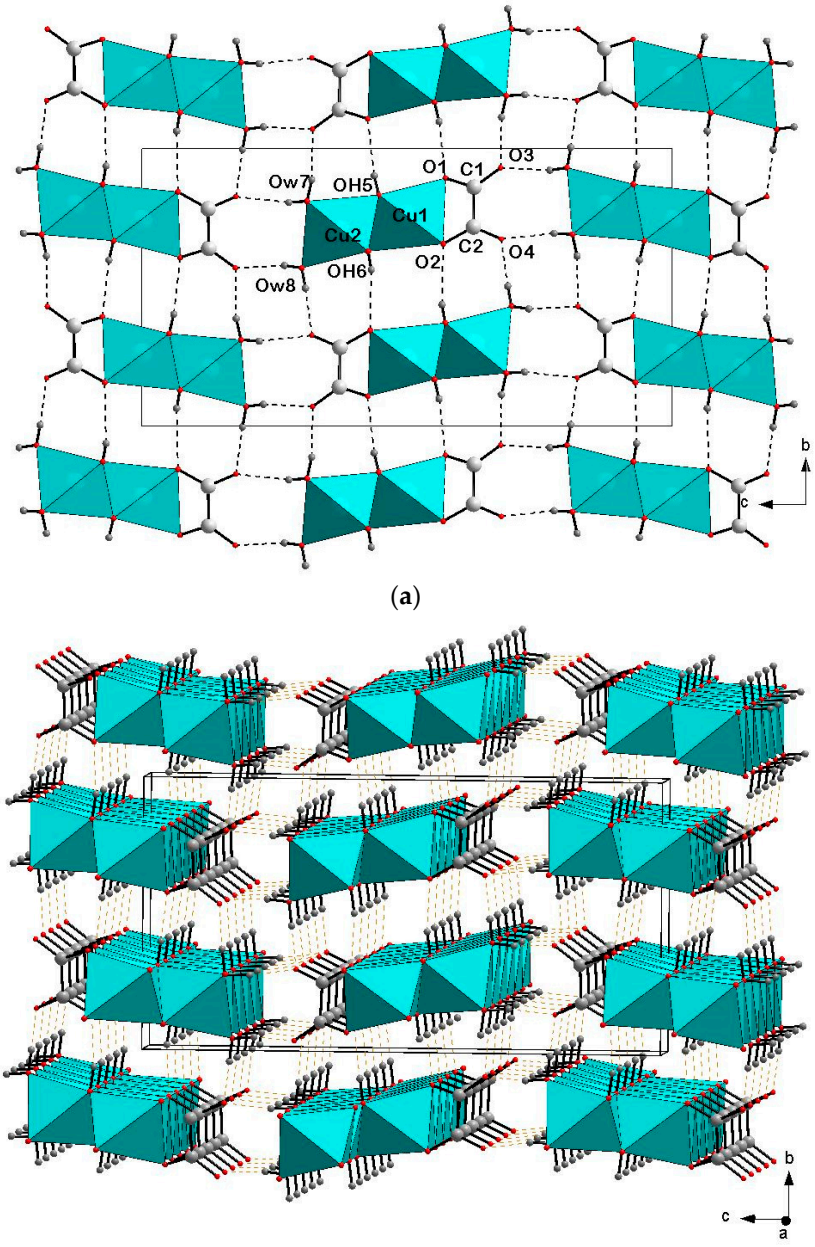

Figure 3. Projection along [100] with atoms labelling (**a**) and perspective view (**b**) of the crystal structure of fiemmeite with hydrogen bonds represented as dashed lines.

A portion of the polymeric rows with composition $[Cu_2(C_2O_4)(OH)_2 \cdot 2H_2O]_n$ is reported in Figure 4a and can be compared with those observed in the structure of middlebackite (Figure 4b). In fiemmeite, the oxalate anion acts as a chelating bidentate ligand with only one of the two independent copper ions, whereas in middlebackite the same anion is tetradentate, acting as a bridge between dimeric octahedral copper units, to form rows extending along [101]. In middlebackite, these rows are interconnected to form channels where the hydroxyl hydrogens are located.

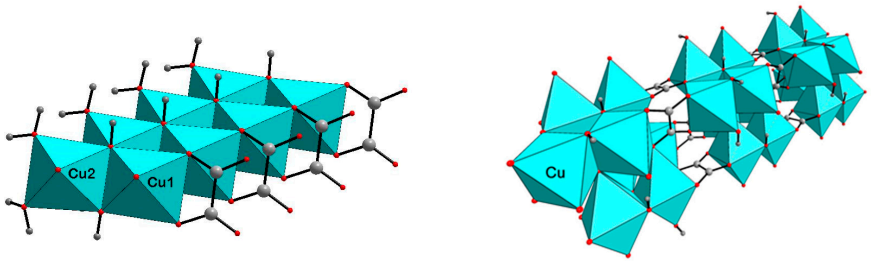

(**a**) (**b**)

Figure 4. Portions of the polymeric rows observed in fiemmeite (**a**) and middlebackite (**b**).

No structural relationships to the other copper-containing oxalates or synthetic compound has been established. In fact, the crystal structure of the synthetic analogue of wheatleyite consists of columns of Cu-centered edge-sharing square bipyramids running along [100] (*a* axis 3.6 Å) and corrugated layers of seven-coordinate Na-centered polyhedra, held together by the oxalate anions and H bonds of water molecules in the vertices of Na-centered polyhedra. In antipinite, columns of edge sharing Cu-centered bipyramids running along [100] are instead combined into a layer by pairs of other Cu bipyramids.

Fiemmeite belongs to class 50.01.06 in the New Dana classification (Salts of Organic Acids, Oxalates) and to 10.AB (Oxalates) in the Nickel–Strunz classification [18].

Supplementary Materials: The CIF file of fiemmeite is available online at http://www.mdpi.com/2075-163X/8/6/248/s1.

Author Contributions: I.R. made the Raman measurements that allowed to discover the new mineral. F.D. performed the diffraction experiments and structure solution. P.F. and I.C. performed the chemical analyses and the determination of the mineral properties. P.F. and I.R. collected most of the material studied.

Funding: This research was funded by Euregio Science Fund (call 2014, IPN16) of the Europaregion Euregio; project "The end-Permian mass extinction in the Southern and Eastern Alps: extinction rates vs. taphonomic biases in different depositional environments".

Acknowledgments: The authors thank the Department of Innovation, Research and University of the Autonomous Province of Bozen/Bolzano for covering the Open Access publication costs. Stefano Dallabona is gratefully thanked for having donated some specimens for study. We also thank Alessandro Guastoni for having provided us with the Raman Spectrum of moolooite from Monte Cervandone and three anonymous referees for useful suggestions.

Conflicts of Interest: The authors declare no conflict of interest.

Appendix A

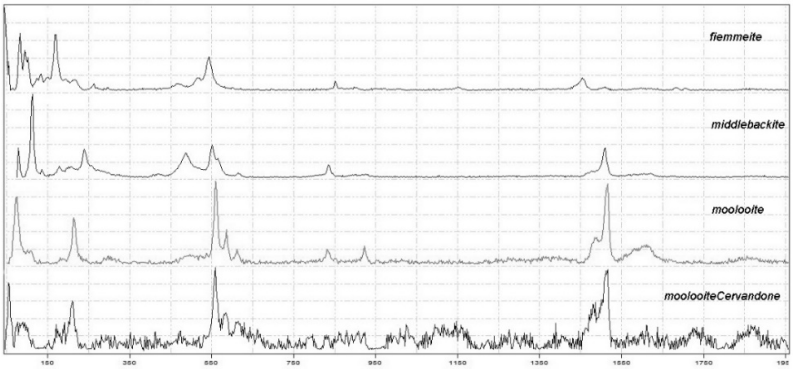

Figure A1. A comparison of the Raman spectra of fiemmeite, middlebackite and moolooite from Passo di San Lugano and moolooite from Monte Cervandone, Val d'Ossola, Italy.

References

1. Massari, F.; Neri, C.; Pittau, P.; Fontana, D.; Stefani, C. Sedimentology, Palynostratigraphy and sequence stratigraphy of a continental to shallow-marine rift-related succession: Upper Permian of the eastern Southern Alps (Italy). *Mem. Sci. Geol. Padova* **1994**, *46*, 119–243.
2. Wopfner, H.; Drake-Brockman, J. Base metal and uranium mineralization in the Groeden Sandstone of South Tyrol. *Geo. Alp* **2017**, *14*, 11–23.
3. Demartin, F.; Campostrini, I.; Ferretti, P.; Rocchetti, I. Second global occurrence of middlebackite near the Passo di San Lugano (Carano, Trento, Italy). *Geo. Alp* **2017**, *14*, 35–38.
4. Elliott, P. Middlebackite, IMA 2015-115. CNMNC Newsletter No. 30, April 2016, page 411. *Mineral. Mag.* **2016**, *80*, 407–413.
5. Mandarino, J.A. The Gladstone-Dale relationship I. Derivation of new constants. *Can. Mineral.* **1976**, *14*, 498–502.
6. Mandarino, J.A. The Gladstone-Dale relationship IV. The compatibility concept and its applications. *Can. Mineral.* **1981**, *19*, 441–450.
7. Frost, R.L. Raman spectroscopy of natural oxalates. *Anal. Chim. Acta* **2004**, *517*, 207–214. [CrossRef]
8. Libowitzky, E. Correlation of O-H stretching frequencies and O-H . . . O hydrogen bond lengths in minerals. *Monatsh. Chem.* **1999**, *130*, 1047–1059.
9. Holland, T.J.B.; Redfern, S.A.T. Unit cell refinement from powder diffraction data: The use of regression diagnostics. *Mineral. Mag.* **1997**, *61*, 65–77. [CrossRef]
10. Sheldrick, G.M. *SADABS Area-Detector Absorption Correction Program*; Bruker AXS Inc.: Madison, WI, USA, 2000.
11. Altomare, A.; Burla, M.C.; Camalli, M.; Cascarano, G.L.; Giacovazzo, C.; Gagliardi, A.; Moliterni, A.G.; Polidori, G.; Spagna, R. SIR97, a new tool for crystal structure determination and refinement. *J. Appl. Crystallogr.* **1999**, *32*, 115–119. [CrossRef]
12. Sheldrick, G.M. Crystal structure refinement with SHELXL. *Acta Crystallogr. C Struct. Chem.* **2015**, *71*, 3–8. [CrossRef] [PubMed]
13. Fischer, R.X.; Tillmanns, E. The equivalent isotropic displacement factor. *Acta Crystallogr. Sect. C Cryst. Struct. Commun.* **1988**, *44*, 775–776. [CrossRef]
14. Brown, I.D. Recent developments in the methods and applications of the Bond Valence Model. *Chem. Rev.* **2009**, *109*, 6858–6919. [CrossRef] [PubMed]
15. Clarke, R.M.; Williams, I.R. Moolooite, a naturally occurring hydrated copper oxalate from western Australia. *Mineral. Mag.* **1986**, *50*, 295–298. [CrossRef]
16. Rouse, R.C.; Peacor, D.R.; Dunn, P.J.; Simmons, W.B.; Newbury, D. Wheatleyite, $Na_2Cu(C_2O_4)_2{\cdot}2H_2O$, a natural sodium copper salt of oxalic acid. *Am. Mineral.* **1986**, *71*, 1240–1242.
17. Chukanov, N.V.; Aksenov, S.M.; Rastsvetaeva, R.K.; Lyssenko, K.A.; Belakovskiy, D.I.; Färber, G.; Möhn, G.; Van, K.V. Antipinite, $KNa_3Cu_2(C_2O_4)_4$, a new mineral species from guano deposits at Pabellón de Pica, Chile. *Mineral. Mag.* **2014**, *78*, 797–804. [CrossRef]
18. Smith, D.G.W.; Nickel, E.H. A system for codification for unnamed minerals: Report of the Subcommittee for Unnamed Minerals of the IMA Commission on New Minerals, Nomenclature and Classification. *Can. Mineral.* **2007**, *45*, 983–1055. [CrossRef]